applied sciences

MDPI

Article

Research Progress on the Microfracture of Shale: Experimental Methods, Microfracture Propagation, Simulations, and Perspectives

Jianyong Zhang [1,2], Zhendong Cui [3,4,5,*], Xiaopeng Chen [6] and Longfei Li [7]

1 College of Geological Engineering, Institute of Disaster Prevention, Sanhe 065201, China; zhangjianyong@cidp.edu.cn
2 Hebei Key Laboratory of Earthquake Disaster Prevention and Risk Assessment, Sanhe 065201, China
3 Key Laboratory of Shale Gas and Geoengineering, Institute of Geology and Geophysics, Chinese Academy of Sciences, Beijing 100029, China
4 Innovation Academy for Earth Science, Chinese Academy of Sciences, Beijing 100029, China
5 College of Earth and Planetary Sciences, University of Chinese Academy of Sciences, Beijing 100049, China
6 Fujian Xiamen Institute of Geological Engineering, Xiamen 361008, China; chenxiaopengxmdz@126.com
7 College of Energy and Mining Engineering, Shandong University of Science and Technology, Qingdao 266590, China; lilongfei@sdust.edu.cn
* Correspondence: cuizhendong@mail.iggcas.ac.cn

Abstract: The fracture network generated by hydraulic fracturing in unconventional shale reservoirs contains numerous microfractures that are connected to macroscopic fractures. These microfractures serve as crucial pathways for shale gas to flow out from micro- and nano-scale pores, playing a critical role in enhancing shale gas recovery. Currently, more attention is being given by academia and industry to the evolution of macroscopic fracture networks, while the understanding of the microfracture mechanisms and evolution is relatively limited. A significant number of microfractures are generated during the hydraulic fracturing process of shale. These microfractures subsequently propagate, merge, and interconnect to form macroscopic fractures. Therefore, studying the fracture process of rock masses from a microscale perspective holds important theoretical significance and engineering value. Based on the authors' research experience and literature review, this paper provides a brief overview of current progress in shale microfracture research from five aspects: in situ observation experiments of microfractures in shale, formation and evolution processes of discontinuous microfractures, the impact of inhomogeneity on microfracture propagation, measurement methods for microscale mechanical parameters and deformation quantities in shale, and numerical simulation of shale microfractures. This paper also summarizes the main challenges and future research prospects in shale microfracture studies, including: (1) quantitative characterization of in situ observation experimental data on shale microfractures; (2) formation and evolution laws of macroscopic, mesoscopic, and microscopic multi-scale discontinuous fractures; (3) more in-depth and microscale characterization of shale heterogeneity and its deformation and fracture mechanisms; (4) acquisition of shale micro-mechanical parameters; (5) refinement and accuracy improvement of the numerical simulation of microfractures in shale. Addressing these research questions will not only contribute to the further development of microfracture theory in rocks but also provide insights for hydraulic fracturing in shale gas extraction.

Keywords: shale; microfractures; microfracture test; discontinuous fracture; heterogeneity; micro mechanical parameters; numerical simulation; challenges and prospects

Citation: Zhang, J.; Cui, Z.; Chen, X.; Li, L. Research Progress on the Microfracture of Shale: Experimental Methods, Microfracture Propagation, Simulations, and Perspectives. *Appl. Sci.* **2024**, *14*, 784. https://doi.org/10.3390/app14020784

Academic Editor: Nikolaos Koukouzas

Received: 11 December 2023
Revised: 11 January 2024
Accepted: 13 January 2024
Published: 17 January 2024

1. Introduction

The extraction of natural gas from shale presents a highly promising and environmentally sustainable alternative to traditional fuel sources [1]. Shale gas, known for its relatively low carbon emissions, possesses the potential to address escalating global energy requirements. Therefore, the development of advanced shale gas extraction technologies has emerged as a prominent subject at the forefront of scientific and technological advancements [2,3]. In order to efficiently extract shale gas from micro- and nano-scale gas-containing pores and fractures (Figure 1), hydraulic fracturing is required for shale reservoirs. The fracture network generated by hydraulic fracturing in shale reservoirs contains numerous microfractures. These microfractures serve as crucial pathways, allowing shale gas to flow from micro- and nano-scale pores towards macroscopic fracturing fractures and wellbores, thereby significantly improving the shale gas recovery rate [4–6]. However, the current academic and industrial focus is primarily on the evolution laws and affected volume of macroscopic fracturing networks, with less attention given to the microfractures connected to these macroscopic fracturing fractures [7,8]. As a result, there is a lack of in-depth understanding regarding their formation mechanisms, distribution characteristics, and dynamic propagation processes, which severely limits breakthroughs in improving shale gas recovery processes [9–11]. Therefore, an in-depth exploration of the causes, characteristics, and propagation patterns of the microfractures generated during the process of hydraulic fracturing in shale holds urgent engineering practicality and significant research value.

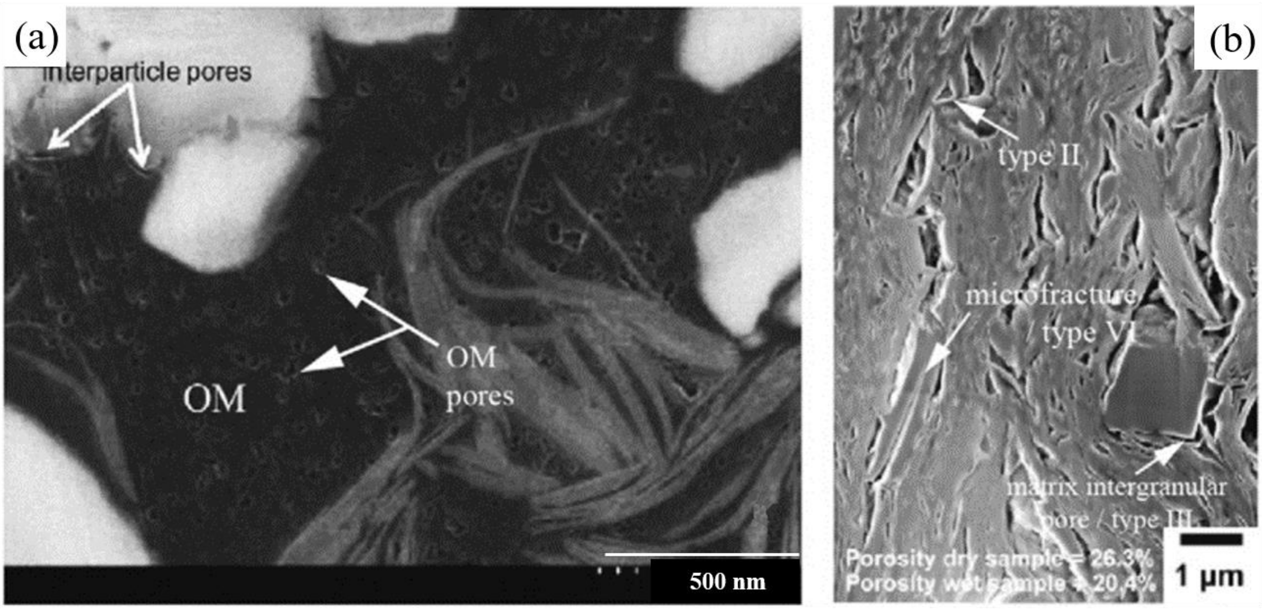

Figure 1. (**a**) Organic matter pores in shale. (**b**) Microfractures connected to gas containing pores [12].

In addition to its practical significance in enhancing shale gas recovery [13], the investigation of microfracturing in rocks holds equal importance for the development of rock fracture theories. The theory of structural control in rock masses posits that the influence of rock mass structure on rock fracturing is significantly greater than that of rock materials, serving as a fundamental theory in rock mechanics. The microfracturing of rocks is similarly influenced by microstructural features such as mineral distribution, porosity, joints, cleavage, and fractures. Within rock masses, there exist abundant microstructures and microfractures, which, upon experiencing stress, undergo processes of extension, merging, and bridging, ultimately resulting in macroscopic fractures [14,15]. Therefore, to gain in-depth insights into the fracture mechanisms of rock masses, the study of rock fracture processes from a microscopic perspective is imperative.

Compared to the research on macroscopic cracks, there has been relatively limited investigation into microfractures in shale, and the mechanisms behind microfracture formation remain unclear. The current state of research in this field is fragmented and lacks a systematic approach, with a dearth of comprehensive review articles outlining the progress made in the study of microfracturing in shale. Experimental testing serves as a fundamental means to conduct research, and the observation of microfractures in shale after hydraulic fracturing, as well as the continuous dynamic monitoring of microfracture initiation and extension in situ, have confirmed that shale fracturing occurs through the generation and connection of discontinuous fractures [16,17]. What are the formation and evolution mechanisms of discontinuous fractures? What factors influence the generation of discontinuous fractures? How does the heterogeneity within shale affect the initiation and propagation of discontinuous fractures? In-depth studies on these issues require the acquisition of the micro-mechanical parameters of shale and the measurement of displacement, deformation, and energy during loading. Hindered by experimental equipment and techniques, satisfactory solutions to these problems have not yet been achieved [18–21]. Therefore, numerous numerical models based on the microstructural distribution have been developed in current research to investigate the initiation and evolution of microcracks [22–24].

Drawing upon the authors' research experience and analysis of existing literature, this paper provides a comprehensive overview of the current research progress in the following five aspects: in situ observation experiments of microfractures in shale, the formation and evolution processes of discontinuous microfractures, the impact of inhomogeneity on microfracture propagation, measurement methods for microscale mechanical parameters and deformation quantities in shale, and numerical simulation of shale microfractures. Additionally, this paper highlights the current challenges and proposes future research directions in this field.

2. In Situ Observation Experiment of Shale Microfractures

In order to investigate the microfracture characteristics of shale, some studies have conducted static observation experiments on microfractures in shale after fracturing [16,25–27]. However, merely observing post-fracture microfractures cannot reflect the influence of the loading process on them, nor can it reveal the initiation and extension process of microfractures in shale. Continuous and dynamic observation of the propagation characteristics of microfractures is necessary in order to obtain a clear and comprehensive understanding of the fracture propagation process and discover general rules [17,28,29].

Currently, there are several in situ observation techniques available for continuously and dynamically observing microfracturing in shale, including optical microscopy with an in situ loading stage, scanning electron microscopy (SEM), and computer tomography (CT) scanning (Figure 2). In situ compression experiments were conducted under an optical microscope to observe the initiation and propagation process of microfractures [30]. However, the low magnification of optical microscopy cannot represent the formation and evolution characteristics of microfractures. SEM equipped with an in situ mechanical loading device has made it possible to dynamically observe microfractures. Some studies have used SEM to observe the continuous propagation process of main fractures and branch fractures in shale and analyze their fracture toughness [17,28]. In addition to SEM, some studies have utilized micro-CT to conduct in situ loading experiments on shale at the microscopic level, observing the generation of extensive microfractures. As the load increases, these microfractures either connect with the main fracture or form new fractures independently [31]. With the advancement of testing methods, some studies have also employed advanced instruments such as positron emission tomography–computed tomography (PET-CT) and high-energy CT to carry out experimental studies on the extension of micro-fractures [32,33].

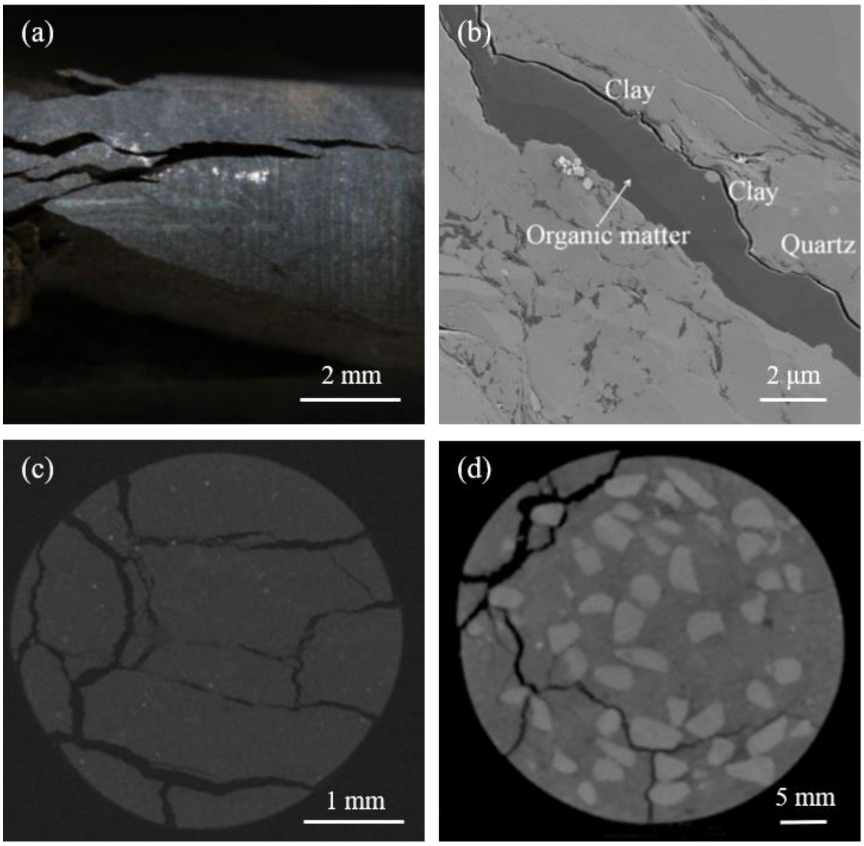

Figure 2. In situ observation experiment of shale microfractures. (**a**) In situ fracture experiment under an optical microscope [30]. (**b**) In situ fracture experiment under scanning electron microscopy [6]. (**c**) In situ fracture experiment under micro-CT [31]. (**d**) In situ rupture experiment under high-energy CT [33].

The aforementioned in situ experiments have successfully observed the dynamic process of microfracture initiation and propagation. Microfractures are typically discontinuous and widely generated. As the load increases, these discontinuous fractures connect with each other to form the main fracture and also generate branch fractures connected to the main fracture, while microfractures that are not connected to the main fracture eventually close [7,16,17,34–39]. What are the mechanisms behind the formation and evolution of these discontinuous microcracks?

3. Research on the Formation and Evolution of Discontinuous Microfractures

3.1. Macroscopic Discontinuous Fractures

The study of unconnected, discontinuous fractures can be traced back to the macroscopic scale, where scholars extensively research natural phenomena such as en echelon faults, segmented fractures, and en echelon vein array (Figure 3) [40–42]. Early studies investigated the generation and evolution mechanisms of en echelon faults at the macroscopic scale based on exposed joints, fissures, and fault zones [43]. With advancements in experimental testing techniques, some studies have conducted research on the connecting process of discontinuous fractures within rocks to explore the mechanisms and precursory characteristics of earthquakes [44–46].

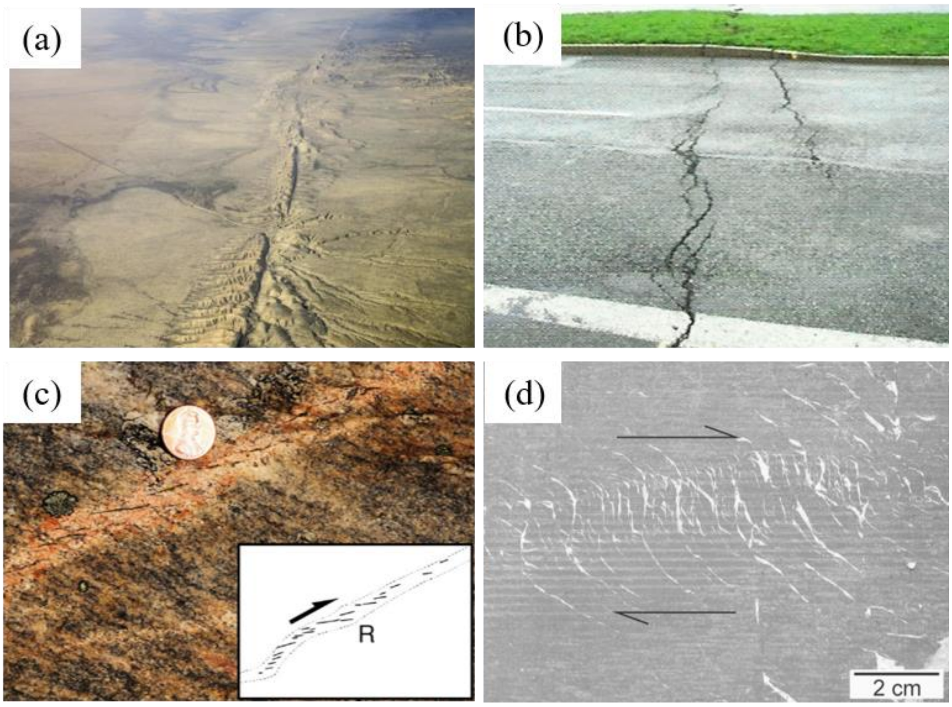

Figure 3. Macroscopic discontinuous fractures. (**a**) Aerial photographs of discontinuous en echelon faults. Credit: US Geological Survey. (**b**) Discontinuous fractures on the road surface [47]. (**c**) Discontinuous fractures forming during incipient stages of faulting [48]. (**d**) En echelon vein array in claystone [49].

3.2. Microscopic Discontinuous Fractures

For the entire continental crust, faults can be considered as microfractures, and the study of en echelon faults can provide a cross-scale reference for understanding microscopic discontinuous fractures. However, the generation, evolution, and mechanical mechanisms of micro-discontinuous fractures still lack a comprehensive explanation. The current consensus is that the formation of discontinuous fractures is influenced by the heterogeneity of shale mechanical strength and complex stress fields, including factors such as porosity, fractures, discontinuity planes, and mineral composition [17,35]. However, these viewpoints lack quantitative evidence from in situ loading experiments.

There has been significant research on the connection forms of discontinuous fractures, and researchers have made good progress in summarizing them [50–52]. The research mainly focuses on the connection process of pre-existing fractures within rocks, including tension fracture connection, shear-driven tensile fracture connection, shear fracture connection, mixed-mode fracture connection, and non-direct connection [53–55]. Most of this research on the connection forms of discontinuous fractures is based on observations of fractured microscale rock samples, with limited research on in situ fracture propagation at the microscopic scale. Therefore, further investigations are needed to study and validate the connection forms of microscale discontinuous fractures.

Microscopic discontinuous fractures exhibit hierarchical distributions, and researchers have summarized the hierarchical distribution characteristics of microfractures through in situ scanning electron microscope tests (Figure 4) [17,34,56]. The spatial distribution of microfractures follows a power law distribution and exhibits self-affinity and hierarchical structure. Based on the evolution of micro-damage and the progressive process of fracturing, laws for multiscale fracture propagation have been proposed, considering the geometric evolution characteristics of fractures in a multiscale damage power law model [27,57]. Currently, the hierarchical distribution characteristics of discontinuous fractures are mostly statistically significant, and hypotheses and numerical simulations are used to explain their formation mechanisms [15,35,58]. Further in situ observation experiments are required to validate these conclusions.

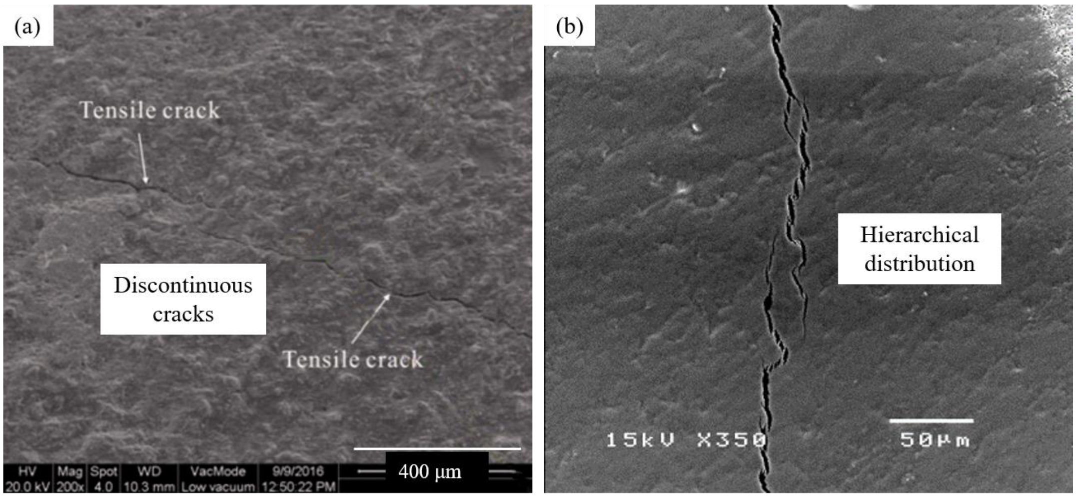

Figure 4. (**a**) Microscopic discontinuous fractures [7]. (**b**) The hierarchical distribution of microscopic discontinuous fractures [34].

4. The Impact of Inhomogeneity on Microfracture Propagation

The mechanism for the formation of discontinuous fractures is attributed to the combined effect of rocks' internal heterogeneity and complex stress fields. The heterogeneity of rocks is mainly manifested in mineral distribution, pores, joints, cleavages, and fissures. Among them, mineral heterogeneity represents the most fundamental type of heterogeneity in rock materials. Different minerals exhibit distinct mechanical properties at their boundaries, and variations in mineral distribution and geometric morphology also exert diverse influences on the process of microfracture propagation.

(1) Intergranular fractures and transgranular fractures

Some studies have investigated the differences between transgranular fractures and intergranular fractures during the loading process, and some of the major findings are as follows [16,26,39,59]. In tensile loading, over 90% of the tensile fractures exist in the form of intergranular fractures, while the remaining 10% exhibit transgranular fractures. In shear loading, the proportion of transgranular fractures increases but still does not exceed 50% [26,39]. Regarding the distribution of microfractures, transgranular fractures in shear loading tend to be closer to the shear centerline, with fewer transgranular fractures as the distance from the shear centerline increases [16,59]. It is evident that the mechanical properties of mineral boundaries are relatively low. Therefore, compared to propagating through mineral grains, fractures are more prone to initiate and propagate along mineral boundaries (Figure 5). However, there are variations in the occurrence of transgranular and intergranular fracture phenomena depending on the loading conditions.

(2) Fracture modes of minerals

The propagation of fractures within different minerals exhibits variations in fracture modes. Microfractures are more prone to propagate in mechanically weaker clay minerals, predominantly through tensile fracture. Conversely, in mechanically stronger minerals such as feldspar and quartz, microfracture formation is less frequent, with shear fracture being the dominant mode [25,60]. Additionally, there are significant differences in the fractal dimension and morphology of microfractures after fracture among different minerals. These variations arise from the distinct mechanical response characteristics and mechanisms of different minerals [57]. Similarly to macroscopic fracture propagation, the differences in mechanical properties between minerals influence the expansion of microfractures (Figure 5).

(3) The influence of mineral geometric morphology and distribution on microfractures

The geometric morphology and distribution of minerals have a significant influence on the generation of microfractures. Scanning electron microscopy observations of microfractures in shale reveal that the distribution of minerals affects the distribution of tensile stress, thereby influencing the location of tensile microfracture initiation [61]. Numerical simulations further confirm that the size of mineral particles also impacts stress distribution, thus influencing the mechanisms underlying microfracture formation [62,63]. Moreover, the morphology and distribution of minerals also exert an influence on the connectivity patterns of microfractures [64]. Essentially, the geometric morphology and distribution of minerals affect stress distribution, thereby influencing the generation and propagation of microfractures.

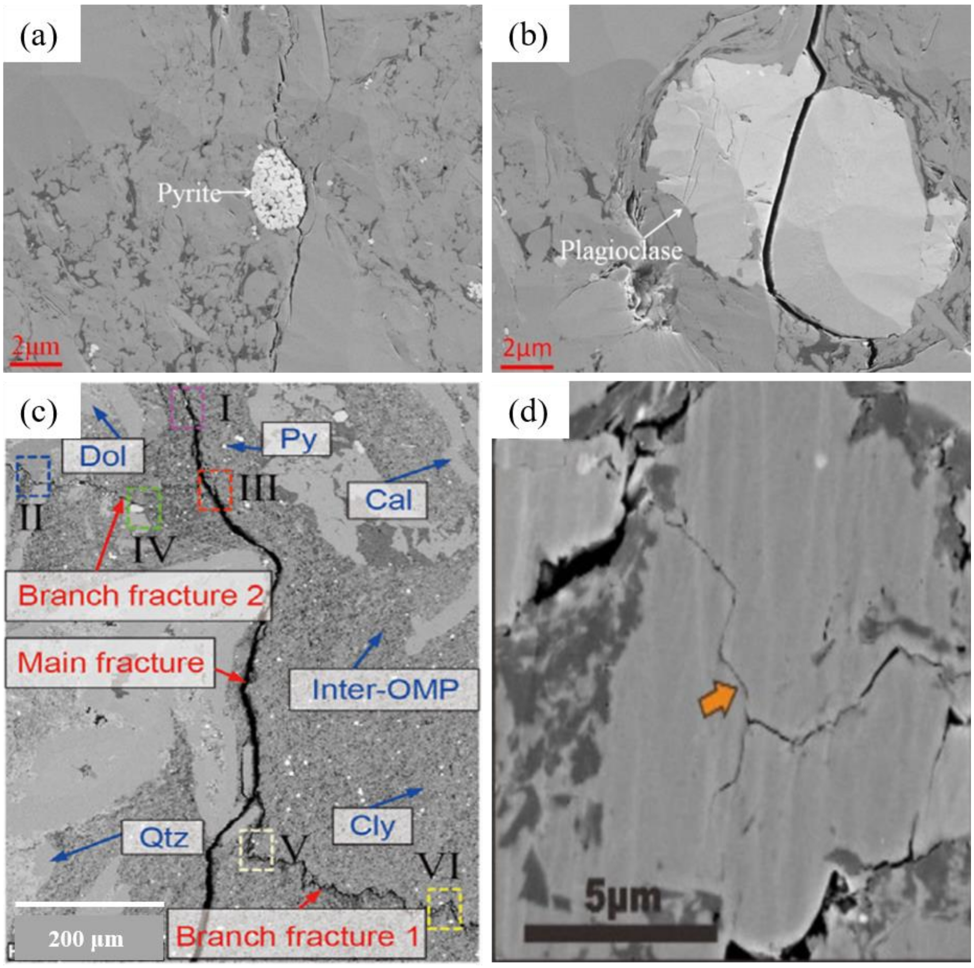

Figure 5. Microfractures in different minerals. (**a**) Due to the higher mechanical properties of pyrite, fractures are unable to propagate through it. Therefore, fractures tend to extend along the boundaries of pyrite [6]. (**b**) In comparison to pyrite, the mechanical properties of plagioclase are lower, allowing fractures to directly propagate through the mineral [6]. (**c**) Fractures tend to propagate along the boundaries of minerals with lower mechanical strength, as well as within clay minerals that have the second lowest mechanical strength. Py = pyrite, Qtz = quartz, Dol = dolomite, Cal = calcite, Cly = clays, Inter-OPM = internal microscopic pore [36]. (**d**) Clay minerals exhibit lower mechanical strength, making them more prone to the formation of complex microfractures [65].

(4) The influence of natural bedding and fractures within shale on microfractures

The anisotropy of shale, which is caused by variations in its microscopic structures, has a direct impact on the propagation of microfractures [66–69]. By integrating fracture mechanics and damage theory, it has been established that the distribution and orientation of microstructures are the primary factors influencing the anisotropy of shale fracture toughness. Additionally, there is a strong correlation between the thickness and inclination angle of bedding and fractures, as well as the initiation and evolution processes of microfractures [70–72]. The degree of consolidation and the mechanical properties of bedding planes also affect the generation and propagation of microfractures [73]. Therefore, it can be inferred that the influence of microscale discontinuities on the propagation of microfractures in shale exhibits similarities to the mechanisms underlying macrofracture generation.

However, the previous experimental studies on shale heterogeneity, apart from numerical simulations, have not considered the mechanical parameters and deformation characterization of minerals, fractures, and discontinuities. These studies have solely provided static observations of microfractures. Incorporating mineral distribution, mineral calibration, interface mechanical parameter acquisition, strain measurement, and fracture path overlay into experiments would greatly advance research on the effects of heterogeneity on the generation and propagation of microfractures.

5. The Measurement Methods for Microscale Mechanical Parameters and Deformation Quantities in Shale

The quantitative measurement of microscale mechanical parameters and deformation quantities in shale is of significant importance for studying the microfracture behavior in shale during loading processes. This section presents a comprehensive overview of the existing methods for quantitatively obtaining microscale mechanical parameters and deformation measurements in shale.

5.1. Measurement of Microscale Mechanical Parameters in Shale

Shale, as a heterogeneous material with complex microstructures and mineral compositions, exhibits deformation and fracture characteristics closely related to mineral distribution and structure. Therefore, obtaining microscale mechanical parameters is fundamental for studying microfracture propagation in shale. Currently, nanoindentation technology and atomic force microscopy (AFM) are widely employed for testing the microscale mechanical properties of shale (Figure 6) [74,75]. Nanoindentation technology involves real-time monitoring of the penetration of an indenter into the material, allowing for the calculation of parameters such as elastic modulus, hardness, fracture toughness, and creep coefficient from the displacement-load curves. AFM, on the other hand, scans the surface of the test sample using a probe fixed on a microcantilever and measures the position changes of the microcantilever through optical detection or tunneling current detection. This provides information about the surface morphology and mechanical properties of the sample. A comparison between nanoindentation technology and AFM testing results in shale revealed that AFM yielded superior results. This is due to the large contact area in nanoindentation technology, while AFM offers nanoscale measurement precision and captures more comprehensive information [76].

The mechanical mode of atomic force microscopy (AFM) provides a means to map the modulus distribution of interfacial phases by generating numerous force-displacement curves, which characterize the variation in modulus across interfaces and phases. By connecting AFM probes to predetermined molecular structures and employing corresponding test substrates, the adhesion forces between molecules and nanoscale particles can be quantified. This technique has been successfully applied in various fields including nanocomposites, biological cell materials, and protein enzymes, for characterizing the adhesive forces between two media [77]. In the field of geotechnical engineering, some studies have utilized AFM to measure the interaction forces between coal particles and the elastic modulus field at micro and nanoscale levels [78,79]. The subsequent application of this method to characterize the adhesive forces between different mineral crystals and between grains with different crystal orientations will advance the theoretical understanding of shale mineral interface phases.

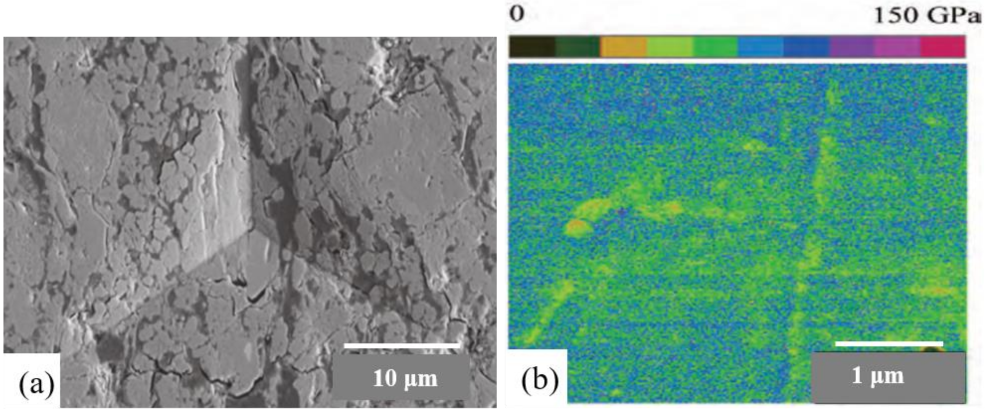

Figure 6. (**a**) Shale nanoindentation testing [80]. (**b**) The distribution of Young's modulus of potassium feldspar measured by AFM [81].

5.2. In Situ Strain Measurement Method for Shale

In macroscopic rock mechanics experiments, strain gauges and displacement sensors are commonly employed to quantitatively characterize the deformation process of rocks, providing insights into their fracturing mechanisms based on the evolution of strain [82,83]. However, in the microscopic domain, how can strain information be obtained quantitatively while microfractures are propagating? This poses a challenge as traditional measurement techniques such as strain sensors cannot be used due to the inability to cover the sample surface during in situ observation of fracture propagation.

Currently, the main methods for microscale strain characterization include digital image correlation (DIC) and electron backscatter diffraction (EBSD) techniques [84,85]. DIC is a non-contact strain measurement technique that has been widely used in various fields such as medicine, materials science, and aerospace due to its wide application range and high precision. In the field of macroscopic rock mechanics experiments, DIC has been extensively applied to measure the deformation and strain during rock fracturing processes, and theoretical analyses have been conducted [86–88]. However, applying this method in microscale rock mechanics experiments presents some challenges. If the rock surface is left untreated and only relies on natural speckles, it may result in low contrast, leading to insufficient accuracy in calculating the strain field [89]. Using traditional black and white spray coatings during the speckle production process can result in larger and unevenly distributed particles. This restricts the use of high magnification scanning electron microscopy (SEM) observation, making it difficult to obtain accurate microscale strain information at high magnifications (Figure 7) [90,91]. In addition to SEM, some researchers have attempted to combine computed tomography (CT) with DIC to quantitatively analyze the initiation, closure, shear, and accumulation features of microfractures in rocks during different loading stages. However, this study still relies on natural speckles on the rock surface, resulting in less accurate strain information [92].

Electron backscatter diffraction (EBSD) is a technique used for point-by-point and line-by-line automated orientation measurements on the surface of a sample, with the acquired data stored [93]. By combining the coordinates of each point in the sample coordinate system and using crystal orientation as imaging criteria, image reconstruction known as orientation imaging microscopy can be achieved. Characterizing and quantitatively analyzing crystal orientation changes during crystal deformation processes contribute to a deeper understanding of the inherent connection between plastic deformation behavior and the initiation and propagation of microfractures. When materials undergo plastic deformation, dislocations are generated within the crystals, along with low-angle dislocation boundaries. Although EBSD cannot directly observe dislocations, it can measure orientation changes caused by a large number of crystal dislocations, and the extent of these changes (misorientation) reflects the degree of crystal deformation. Specifically, this orientation change can be studied through Euler angles, pattern quality, small angle grain boundaries, inverse pole figures, and misorientation [94]. Quantitative characterization of crystal deformation behavior can be achieved by studying the changes in grain orientation, misorientation angles, and Schmid factor evolution during in situ loading processes. This technique is widely applied in materials science, and in the field of microscale rock deformation. It has only been utilized in tectonic geology to investigate structural deformations in rocks and infer their geological evolution history (Figure 7) [95]. Its application in in situ loading experiments is still limited but holds significant potential for future development.

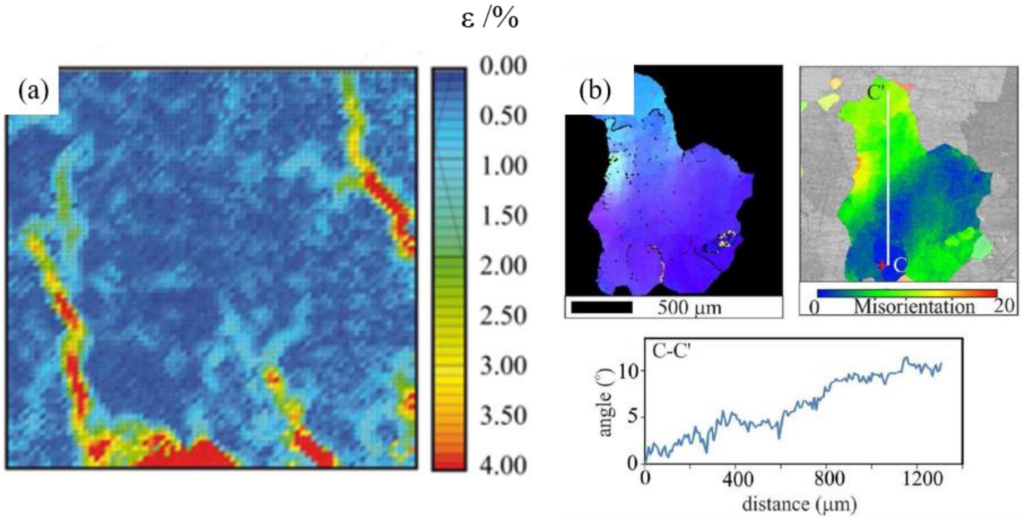

Figure 7. (**a**) Full-field strain measurement using DIC during fracture propagation [91]. (**b**) Using a misorientation angle in EBSD to represent the magnitude of structural strain [95].

6. Microscale Fracture Simulation in Shale

Due to the high difficulty and limited measurement methods of in situ microfracture propagation observation tests, a clear understanding of the microscale fracture propagation behavior cannot be achieved experimentally. However, numerical simulation modeling is flexible and not restricted by experimental conditions, leading to abundant research achievements in related fields. Currently, commonly used fracture propagation simulation methods include discrete element methods and finite element methods [96–101]. In numerical simulations, widely adopted microscale fracture theories in shale include brittle fracture theory, elastic–plastic theory, damage mechanics theory, and microplane constitutive model theory. However, it should be noted that due to the discontinuous, heterogeneous, and anisotropic nature of rock materials, a single constitutive theory is insufficient to comprehensively reflect the microscale fracture behavior of shale.

In order to capture the influence of microstructural features on fracture propagation, various numerical models based on microstructural distributions have been developed. For example, the universal distinct element code (UDEC) particle boundary model [102,103], three-dimensional distinct element code (3DEC)–Voronoi model [104,105], three-dimensional polygon-based discrete element method (DEM) model [106], particle flow code (PFC)–grain based model (GBM) model [107–109], and Irazu–GBM model [110]. Li et al. [22,111] employed the mineral distribution-based finite-discrete element method (FDEM) to investigate the effects of boundary conditions, mineral geometry, and loading rate on the fracture process and the initiation, propagation, and connection of microfractures under uniaxial compression conditions in granite. Lan et al. [15] conducted uniaxial compression experiments based on the UDEC mineral distribution model and found that the nonuniformity of grain size affects the distribution of tensile stress, making rocks with nonuniform grain size more prone to tensile microfractures compared to rocks with uniform grains. Li et al. [106] studied the influence of grain size on microfracture propagation based on the 3D polycrystalline discrete element method (3PDEM) mineral distribution-based finite-discrete element method (FDEM)–Voronoi model and found that when the grain size is larger, fracture propagation along the loading direction is easier, leading to a series of perpendicular tensile failures, while for smaller grain sizes, microfractures are more scattered. Xu et al. [24] established a uniaxial compression experimental model based on the microstructure of coal rock and suggested that mineral interface microfractures are generated due to nonuniform mineral strain, and the formation of tensile microfractures dominates the rock's uniaxial compressive failure behavior. Zhou et al. [60] investigated the proportions of shear and tensile microfractures during uniaxial compression using the PFC–GBM model. Saadat et al. [63] studied the formation and propagation processes of microfractures in shear bands under different uniaxial compression loads using the cohesive contact model (CCM) in PFC. Based on the methods provided in the aforementioned literature, these models can be conveniently used to model mineral distributions in experiments and conduct mechanical calculations for studying fracture propagation mechanisms and other related aspects (Figure 8).

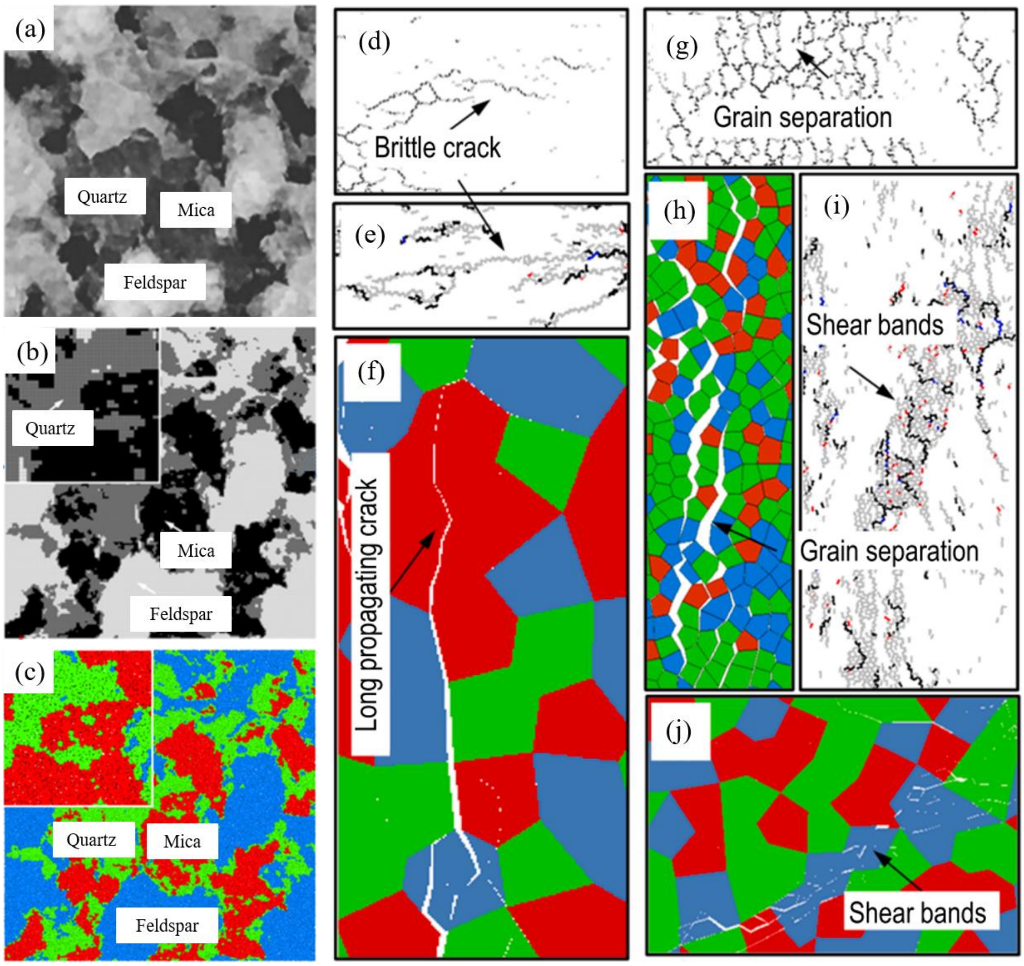

Figure 8. Simulation and modeling of microscale fracture propagation in rock based on mineral distribution. (**a**) Experimental testing of rock mineral distribution. (**b**) Utilizing digital image processing techniques to obtain a grain-based sketch. (**c**) Generating computational models based on sketches within numerical simulation. (**d**–**j**) Simulation of microscale fracture propagation in rock [112].

Despite rapid advancements in experimental techniques, there is still a lack of measurement methods at the microscale level. For instance, the measurement of microscale stresses can be inferred through inverse methods [113–115], but it is difficult to directly measure stress within the microzones of materials. However, the combination of experiments and numerical simulations provides a promising approach for studying microscale fracture propagation and its mechanical mechanisms. By conducting experiments to obtain mechanical properties, mineral distribution, and microstrains during the process of fracture propagation, and subsequently performing targeted numerical simulations, a better understanding of the mechanical mechanisms governing microscale fracture propagation can be achieved [36,116,117].

7. Challenges and Future Perspectives

Based on the literature review, the authors have identified several major challenges in current research on shale microfractures and provided future research prospects. These include:

(1) The difficulty in quantifying experimental data such as strain and energy in in situ observation experiments of shale microfractures. To address this issue, future studies can utilize quantitative research methods such as high-precision acoustic emission and microscale digital image correlation during in situ observation experiments to obtain information on energy and strain during rock fracture processes. In addition, developing thin shale sections for transmission electron microscopy observations can reveal the atomic-scale deformation and fracture mechanisms of shale, thus advancing in situ observation studies.

(2) Limited research on the formation and evolution of non-planar fractures at multiple scales (macro, meso, and micro). More investigations are needed to understand the experimental phenomena, common patterns, and mechanisms involved in fractures at different scales.

(3) In-depth exploration of the definition of microscale heterogeneity and its influence on the initiation and propagation of microfractures in shale. Questions regarding the definition of microscale heterogeneity in shale and the identification of the fundamental elements of heterogeneity at different magnifications have yet to be answered. The advancement of research in constitutive rock relationships and fracture theory will lead to significant changes alongside deeper and more detailed studies. This requires the improvement of experimental techniques and interdisciplinary research collaboration among rock mechanics, materials science, and physics.

(4) Difficulties in obtaining microscale mechanical parameters of shale, leading to a significant lag in research compared to fields such as metals and materials science. The problem of acquiring macro-scale interface mechanical parameters of rocks remains unsolved, and obtaining microscale interface mechanical parameters is even more challenging. If the microscale interface mechanical properties of rocks can be obtained, it would facilitate research on macroscale rock interface issues and further advance rock mechanics theory.

(5) The main challenges in numerical simulation studies of shale microfractures lie in inaccurate microscale mechanical parameters, difficulties in determining boundary conditions, and unclear microfracture criteria. Consequently, numerical simulation studies often rely on assumptions, model simplifications, and other limitations, making it difficult to reach widely accepted conclusions. Despite the short-term difficulty in overcoming these challenges, numerical simulations still play a crucial role in exploring rock fracture theories, qualitative analysis, comparative studies, and visualization presentations.

8. Conclusions

(1) Optical microscopy, scanning electron microscopy, and computer tomography with in situ loading devices are excellent experimental methods for dynamic observation of microfracture propagation in shale. Experimental findings indicate that microfractures in shale mainly propagate through discontinuous fracture initiation and connection. The mechanism behind the generation of discontinuous fractures lies in the internal heterogeneity of shale, including mineral distribution, pore spaces, joints, cleavage, and fissures.

(2) Quantitative measurement of microscale mechanical parameters and deformation quantities in shale plays a crucial role in understanding the behavior of microfractures during loading processes. However, there is still room for improvement in terms of relevant experimental testing methods.

(3) Numerical simulation methods have been developed to study microfracture behavior in shale, leading to significant research achievements. However, their effectiveness can be enhanced by mutual validation with laboratory test results, allowing for a better understanding of the mechanical mechanisms behind microfracture propagation.

Author Contributions: Investigation—L.L.; Resources—X.C.; Writing—J.Z.; Supervision—Z.C. All authors have read and agreed to the published version of the manuscript.

Funding: This work was funded by the Second Tibetan Plateau Scientific Expedition and Research Program (STEP) (Grant No. 2019QZKK0904), the Fundamental Research Funds for the Central Universities (Grant No. ZY20230219), Langfang City Science and Technology Support Plan Project (Grant No. 2023013094), and the National Natural Science Foundation of China (Grant No. 41972296).

Data Availability Statement: Data is contained within the article.

Conflicts of Interest: The authors declare no conflicts of interest.

References

1. Bellani, J.; Verma, H.K.; Khatri, D.; Makwana, D.; Shah, M. Shale gas: A step toward sustainable energy future. *J. Pet. Explor. Prod. Technol.* **2021**, *11*, 2127–2141. [CrossRef]
2. Naumenko-Dèzes, M.; Kloppmann, W.; Blessing, M.; Bondu, R.; Gaucher, E.C.; Mayer, B. Natural gas of radiolytic origin: An overlooked component of shale gas. *Proc. Natl. Acad. Sci. USA* **2022**, *119*, e2114720119. [CrossRef] [PubMed]
3. Whitelaw, P.; Uguna, C.N.; Stevens, L.A.; Meredith, W.; Snape, C.E.; Vane, C.H.; Moss-Hayes, V.; Carr, A.D. Shale gas reserve evaluation by laboratory pyrolysis and gas holding capacity consistent with field data. *Nat. Commun.* **2019**, *10*, 3659. [CrossRef]
4. Curtis, J. Fractured shale-gas systems. *Aapg Bull.* **2002**, *86*, 1921–1938. [CrossRef]
5. Ding, W.; Li, C.; Li, C.; Xu, C.; Jiu, K.; Zeng, W.; Wu, L. Fracture development in shale and its relationship to gas accumulation. *Geosci. Front.* **2012**, *3*, 97–105. [CrossRef]
6. He, J.; Li, X.; Yin, C.; Zhang, Y.; Lin, C. Propagation and characterization of the micro cracks induced by hydraulic fracturing in shale. *Energy* **2020**, *191*, 116449. [CrossRef]
7. Liu, S.; Wang, Z.; Zhang, L. Experimental study on the cracking process of layered shale using X-ray microCT. *Energy Explor. Exploit.* **2017**, *36*, 297–313. [CrossRef]
8. Zhou, J.; Zeng, Y.; Guo, Y.; Chang, X.; Liu, L.; Wang, L.; Hou, Z.; Yang, C. Effect of natural filling fracture on the cracking process of shale Brazilian disc containing a central straight notched flaw. *J. Pet. Sci. Eng.* **2021**, *196*, 107993. [CrossRef]
9. Shang, X.; Long, S.; Duan, T. Fracture system in shale gas reservoir: Prospect of characterization and modeling techniques. *J. Nat. Gas Geosci.* **2021**, *6*, 157–172. [CrossRef]
10. Xu, C.; Kang, Y.; You, Z.; Chen, M. Review on formation damage mechanisms and processes in shale gas reservoir: Known and to be known. *J. Nat. Gas Sci. Eng.* **2016**, *36*, 1208–1219. [CrossRef]
11. Zhao, J.; Ren, L.; Jiang, T.; Hu, D.; Wu, L.; Wu, J.; Yin, C.; Li, Y.; Hu, Y.; Lin, R.; et al. Ten years of gas shale fracturing in China: Review and prospect. *Nat. Gas Ind. B* **2022**, *9*, 158–175. [CrossRef]
12. Ougier-Simonin, A.; Renard, F.; Boehm, C.; Vidal-Gilbert, S. Microfracturing and microporosity in shales. *Earth-Sci. Rev.* **2016**, *162*, 198–226. [CrossRef]
13. Yang, Y.; Zhang, X.; Zhou, X.; Wang, A.; Li, J. Real Gas Effect and Bulk Diffusion Characteristics of Shale Mixed Gas Transport in Microscale Fractures. *ACS Omega* **2023**, *8*, 17077–17085. [CrossRef]
14. Wang, Y.; Feng, W.K.; Zhao, Z.H.; Zhang, D. Anisotropic energy and ultrasonic characteristics of black shale under triaxial deformation revealed utilizing real-time ultrasonic detection and post-test CT imaging. *Geophys. J. Int.* **2019**, *219*, 260–270. [CrossRef]
15. Lan, H.; Martin, C.D.; Hu, B. Effect of heterogeneity of brittle rock on micromechanical extensile behavior during compression loading. *J. Geophys. Res.* **2010**, *115*, 1–20. [CrossRef]
16. Cheng, Y.; Wong, L.N.Y. Microscopic Characterization of Tensile and Shear Fracturing in Progressive Failure in Marble. *J. Geophys. Res. Solid Earth* **2018**, *123*, 204–225. [CrossRef]
17. Cui, Z.; Han, W. In Situ Scanning Electron Microscope (SEM) Observations of Damage and Crack Growth of Shale. *Microsc. Microanal.* **2018**, *24*, 107–115. [CrossRef] [PubMed]
18. Abedi, S.; Slim, M.; Hofmann, R.; Bryndzia, T.; Ulm, F.-J. Nanochemo-mechanical signature of organic-rich shales: A coupled indentation–EDX analysis. *Acta Geotech.* **2016**, *11*, 559–572. [CrossRef]
19. Deirieh, A.; Ortega, J.A.; Ulm, F.J.; Abousleiman, Y. Nanochemomechanical assessment of shale: A coupled WDS-indentation analysis. *Acta Geotech.* **2012**, *7*, 271–295. [CrossRef]
20. Kumar, V.; Curtis, M.E.; Gupta, N.; Sondergeld, C.H.; Rai, C.S. Estimation of Elastic Properties of Organic Matter and Woodford Shale Through Nano-indentation Measurements. In Proceedings of the SPE Canadian Unconventional Resources Conference, Calgary, AB, Canada, 30 October–1 November 2012.
21. Ulm, F.-J.; Abousleiman, Y. The Nanogranular Nature of Shale. *Acta Geotech.* **2006**, *1*, 77–88. [CrossRef]

22. Li, X.; Li, H.; Liu, L.; Liu, Y.; Ju, M.; Zhao, J. Investigating the crack initiation and propagation mechanism in brittle rocks using grain-based finite-discrete element method. *Int. J. Rock Mech. Min. Sci.* **2020**, *127*, 104219. [CrossRef]
23. Liu, X.; Liang, Z.; Meng, S.; Tang, C.; Tao, J. Numerical Simulation Study of Brittle Rock Materials from Micro to Macro Scales Using Digital Image Processing and Parallel Computing. *Appl. Sci.* **2022**, *12*, 3864. [CrossRef]
24. Xu, H.; Wang, G.; Fan, C.; Liu, X.; Wu, M. Grain-scale reconstruction and simulation of coal mechanical deformation and failure behaviors using combined SEM Digital Rock data and DEM simulator. *Powder Technol.* **2020**, *360*, 1305–1320. [CrossRef]
25. Daigle, H.; Hayman, N.; Kelly, E.; Milliken, K.; Jiang, H. Fracture capture of organic pores in shales: Fracture capture of organic pores. *Geophys. Res. Lett.* **2017**, *44*, 2167–2176. [CrossRef]
26. Fujii, Y.; Takemura, T.; Takahashi, M.; Lin, W. Surface features of uniaxial tensile fractures and their relation to rock anisotropy in Inada granite. *Int. J. Rock Mech. Min. Sci.* **2007**, *44*, 98–107. [CrossRef]
27. Zhong, J.; Liu, S.; Ma, Y.; Yin, C.; Liu, C.; Li, Z.; Liu, X.; Li, Y. Macro-fracture mode and micro-fracture mechanism of shale. *Pet. Explor. Dev.* **2015**, *42*, 269–276. [CrossRef]
28. Zuo, J.; Li, Y.; Liu, C.; Liu, H.; Wang, J.; Li, H.; Liu, L. Meso-fracture mechanism and its fracture toughness analysis of Longmaxi shale including different angles by means of M-SENB tests. *Eng. Fract. Mech.* **2019**, *215*, 178–192. [CrossRef]
29. Zuo, J.; Wang, X.; Mao, D. SEM in-situ study on the effect of offset-notch on basalt cracking behavior under three-point bending load. *Eng. Fract. Mech.* **2014**, *131*, 504–513. [CrossRef]
30. Huang, B.; Li, L.; Tan, Y.; Hu, R.; Li, X. Investigating the Meso-Mechanical Anisotropy and Fracture Surface Roughness of Continental Shale. *J. Geophys. Res. Solid Earth* **2020**, *125*, 1–23. [CrossRef]
31. Li, X.; Duan, Y.; Li, S.; Zhou, R. Study on the progressive failure characteristics of Longmaxi shale under uniaxial compression conditions by X-ray micro-computed tomography. *Energies* **2017**, *10*, 303. [CrossRef]
32. Li, S.; Liu, L.; Chai, P.; Li, X.; He, J.; Zhang, Z.; Wei, L. Imaging hydraulic fractures of shale cores using combined positron emission tomography and computed tomography (PET-CT) imaging technique. *J. Pet. Sci. Eng.* **2019**, *182*, 106283. [CrossRef]
33. Sun, X.; Li, X.; Zheng, B.; He, J.; Mao, T. Study on the progressive fracturing in soil and rock mixture under uniaxial compression conditions by CT scanning. *Eng. Geol.* **2020**, *279*, 105884. [CrossRef]
34. Cui, Z.; Li, X.; Liu, D. In-situ observation of en echelon intermittent intermittent cracks of shale in micro-nano scale. *J. Eng. Geol.* **2018**, *26*, 85–90.
35. Tang, H. Multi-scale crack propagation and damage acceleration during uniaxial compression of marble. *Int. J. Rock Mech. Min. Sci.* **2020**, *131*, 104330. [CrossRef]
36. Liu, X.; Meng, S.-W.; Liang, Z.; Tang, C.a.; Tao, J.; Tang, J. Microscale crack propagation in shale samples using focused ion beam scanning electron microscopy and three-dimensional numerical modeling. *Pet. Sci.* **2023**, *20*, 1488–1512. [CrossRef]
37. Han, B.; Yang, H. Microscopic fracture process and quantitative study of shale under different confining pressures. *Coal Sci. Technol.* **2019**, *47*, 90–95.
38. Yang, S.; Xu, T.; He, L.; Jing, H.; Wen, S.; Yu, Q.L. Numerical study on failure behavior of brittle rock specimen containing pre-existing combined flaws under different confining pressure. *Arch. Civ. Mech. Eng.* **2015**, *15*, 1085–1097. [CrossRef]
39. Zhang, J.; Cui, Z.; Han, W.; Si, K.; Zhao, Y. Comparative Study on Mineral-Scale Microcrack Propagation of Shale under Different Loading Methods. *Adv. Civ. Eng.* **2021**, *2021*, 1–18. [CrossRef]
40. Kim, Y.-S.; Peacock, D.C.P.; Sanderson, D.J. Mesoscale strike-slip faults and damage zones at Marsalforn, Gozo Island, Malta. *J. Struct. Geol.* **2003**, *25*, 793–812. [CrossRef]
41. Lajtai, E.Z.; Carter, B.J.; Duncan, E.J.S. En echelon crack-arrays in potash salt rock. *Rock Mech. Rock Eng.* **1994**, *27*, 89–111. [CrossRef]
42. Siad, L.; Megueddem, M. Stability analysis of jointed rock slope. *Mech. Res. Commun.* **1998**, *25*, 661–670. [CrossRef]
43. Tikoff, B.; Teyssier, C. Formation of en-échelon pull-apart arrays in pure-shear dominated transpression. *J. Struct. Geol.* **2022**, *162*, 104675. [CrossRef]
44. Wong, L.N.Y.; Einstein, H.H. Crack Coalescence in Molded Gypsum and Carrara Marble: Part 1. Macroscopic Observations and Interpretation. *Rock Mech. Rock Eng.* **2009**, *42*, 475–511. [CrossRef]
45. Ren, Y.; Liu, P.; Ma, J.; Chen, S. Experimental study on evolution of thermal field of en echelon fault during the meta-instability stage. *Chin. J. Geophys.* **2013**, *56*, 2348–2357.
46. Wang, X.; Ma, J.; Liu, L. Numerical simulation of large shear strain drops during jog failure for echelon faults based on a heterogeneous and strain-softening model. *Tectonophysics* **2013**, *608*, 667–684. [CrossRef]
47. Surowiecki, A.; Saska, P.; Ksiądzyna, K.; Ryczyński, J. Traffic infrastructure in mining areas (selected problems). *Sci. J. Mil. Univ. Land Forces* **2019**, *193*, 558–578. [CrossRef]
48. Fossen, H. Chapter 8-Fault classification, fault growth and displacement. In *Regional Geology and Tectonics*, 2nd ed.; Scarselli, N., Adam, J., Chiarella, D., Roberts, D.G., Bally, A.W., Eds.; Elsevier: Amsterdam, The Netherlands, 2020; pp. 119–147.
49. Tóth, E.; Hrabovszki, E.; Tóth, T.M.; Schubert, F. Shear strain and volume change associated with sigmoidal vein arrays in the Boda Claystone. *J. Struct. Geol.* **2020**, *138*, 104105. [CrossRef]
50. Afolagboye, L.O.; He, J.; Wang, S. Crack Initiation and Coalescence Behavior of Two Non-parallel Flaws. *Geotech. Geol. Eng.* **2018**, *36*, 105–133. [CrossRef]
51. Zhang, P.; Li, N.; He, R.L. Experimental Study on Mechanism of Crack Coalescence between Two Pre-Existing Flaws under Dynamic Loading. *Key Eng. Mater.* **2006**, *324–325*, 117–120. [CrossRef]

52. Bi, J.; Tang, J.; Wang, C.; Quan, D.; Teng, M. Crack Coalescence Behavior of Rock-Like Specimens Containing Two Circular Embedded Flaws. *Lithosphere* **2022**, *2022*, 9498148. [CrossRef]
53. Zhang, X.; Liu, Q.; Wu, S.; Tang, X. Crack coalescence between two non-parallel flaws in rock-like material under uniaxial compression. *Eng. Geol.* **2015**, *199*, 74–90. [CrossRef]
54. Xu, J.; Zheng, Z.; Xiao, X.; Li, Z. Crack propagation and coalescence due to dual non-penetrating surface flaws and their effect on the strength of rock-like material. *J. Geophys. Eng.* **2018**, *15*, 938–951. [CrossRef]
55. Wong, L.N.Y.; Einstein, H.H. Coalescence Behavior In Carrara Marble And Molded Gypsum Containing Artificial Flaw Pairs Under Uniaxial Compression. In Proceedings of the 1st Canada-U.S. Rock Mechanics Symposium, Vancouver, Canada, 27–31 May 2007; p. ARMA–07-071.
56. Chen, J.; Lan, H.; Macciotta, R.; Martin, C.D.; Wu, Y. Microfracture characterization of shale constrained by mineralogy and bedding. *J. Pet. Sci. Eng.* **2021**, *201*, 108456. [CrossRef]
57. Lan, H.; Chen, J.; Wu, Y. Spatial characterization of micro and nanoscale micro-cracks in gas shale before and after triaxial compression test. *J. Eng. Geol.* **2018**, *26*, 24–35.
58. Hallbauer, D.K.; Wagner, H.; Cook, N.G.W. Some observations concerning the microscopic and mechanical behaviour of quartzite specimens in stiff, triaxial compression tests. *Int. J. Rock Mech. Min. Sci. Geomech. Abstr.* **1973**, *10*, 713–726. [CrossRef]
59. Zeng, W.; Ding, W.; Zhang, J.; Zhang, Y.; Ling, G.; Kai, J.; Li, Y. Fracture development in Paleozoic shale of Chongqing area (South China). Part two: Numerical simulation of tectonic stress field and prediction of fractures distribution. *J. Asian Earth Sci.* **2013**, *75*, 267–279. [CrossRef]
60. Zhou, J.; Lan, H.; Zhang, L.; Yang, D.; Song, J.; Wang, S. Novel grain-based model for simulation of brittle failure of Alxa porphyritic granite. *Eng. Geol.* **2019**, *251*, 100–114. [CrossRef]
61. Slatt, R.; O'Brien, N. Pore types in the Barnett and Woodford gas shales: Contribution to understanding gas storage and migration pathways in finegrained rocks. *AAPG Bull.* **2011**, *95*, 2017–2030. [CrossRef]
62. Mahdi, S.; Abbas, T. A numerical approach to investigate the effects of rock texture on the damage and crack propagation of a pre-cracked granite. *Comput. Geotech.* **2019**, *111*, 89–111. [CrossRef]
63. Saadat, M.; Taheri, A. A cohesive grain based model to simulate shear behaviour of rock joints with asperity damage in polycrystalline rock. *Comput. Geotech.* **2020**, *117*, 103254. [CrossRef]
64. Tian, W.; Yang, S.; Xie, L.; Wang, Z. Cracking behavior of three types granite with different grain size containing two non-coplanar fissures under uniaxial compression. *Arch. Civ. Mech. Eng.* **2018**, *18*, 1580–1596. [CrossRef]
65. Han, J.; Zhu, H.; Lu, Y.; Yang, S.; Yang, M.; Shi, E.; Qi, Y. Microstructural Analysis of Organic-Rich Shales: Insights from an Electron Microscopic Study by Application of FIBSEM and TEM. *Nanomaterials* **2022**, *12*, 4135. [CrossRef]
66. Ding, P.; Wang, D.; Gong, F.; Wang, L.; Li, X.-y. Laboratory observation of velocity anisotropy affected by clays and microcracks in artificial clay-rich shale samples. *J. Pet. Sci. Eng.* **2020**, *191*, 107156. [CrossRef]
67. Sui, W.; Wang, Y.; Li, J. Microscopic Study of Shale Anisotropy with SEM In Situ Compression and Three-Point Bending Experiments. *Energies* **2023**, *16*, 2440. [CrossRef]
68. Wang, Y.; Liu, D.; Zhao, Z.; Wang, H. Investigation on the effect of confining pressure on the geomechanical and ultrasonic properties of black shale using ultrasonic transmission and post-test CT visualization. *J. Pet. Sci. Eng.* **2020**, *185*, 106630. [CrossRef]
69. Duan, Y.; Yang, B. How does structure affect the evolution of cracking and the failure mode of anisotropic shale? *Geomech. Geophys. Geo-Energy Geo-Resour.* **2021**, *8*, 25. [CrossRef]
70. Li, C.; Xie, H.; Wang, J. Anisotropic characteristics of crack initiation and crack damage thresholds for shale. *Int. J. Rock Mech. Min. Sci.* **2020**, *126*, 104178. [CrossRef]
71. Nasseri, M.H.B.; Mohanty, B. Fracture toughness anisotropy in granitic rocks. *Int. J. Rock Mech. Min. Sci.* **2008**, *45*, 167–193. [CrossRef]
72. Nasseri, M.H.B.; Mohanty, B.; Young, R.P. Fracture Toughness Measurements and Acoustic Emission Activity in Brittle Rocks. *Pure Appl. Geophys.* **2006**, *163*, 917–945. [CrossRef]
73. Cui, Z.; Qi, S.; Han, W. The role of weak bedding planes in the cross-layer crack growth paths of layered rocks. *Geomech. Geophys. Geo-Energy Geo-Resour.* **2022**, *8*, 22. [CrossRef]
74. Liu, K.; Ostadhassan, M. Microstructural and geomechanical analysis of Bakken shale at nanoscale. *J. Pet. Sci. Eng.* **2017**, *153*, 133–144. [CrossRef]
75. Yang, J.; Hatcherian, J.; Hackley, P.C.; Pomerantz, A.E. Nanoscale geochemical and geomechanical characterization of organic matter in shale. *Nat. Commun.* **2017**, *8*, 1–9. [CrossRef]
76. Li, Y.; Chen, J.-Q.; Yang, J.-H.; Liu, J.-S.; Tong, W.-S. Determination of shale macroscale modulus based on microscale measurement: A case study concerning multiscale mechanical characteristics. *Pet. Sci.* **2022**, *19*, 1262–1275. [CrossRef]
77. Kim, H.; Ishibashi, K.; Matsuo, K.; Kira, A.; Okada, T.; Watanabe, K.; Inada, M.; Nakamura, C. Quantitative Measurements of Intercellular Adhesion Strengths between Cancer Cells with Different Malignancies Using Atomic Force Microscopy. *Anal Chem* **2019**, *91*, 10557–10563. [CrossRef] [PubMed]
78. Liu, J.; Wang, J.; Huang, J.; Cui, X.; Tan, X.; Liu, Q.; Zeng, H. Heterogeneous Distribution of Adsorbed Bitumen on Fine Solids from Solvent-Based Extraction of Oil Sands Probed by AFM. *Energy Fuels* **2017**, *31*, 8833–8842. [CrossRef]
79. Xing, Y.; Li, C.; Gui, X.; Cao, Y. Interaction Forces between Paraffin/Stearic Acid and Fresh/Oxidized Coal Particles Measured by Atomic Force Microscopy. *Energy Fuels* **2017**, *31*, 3305–3312. [CrossRef]

80. Bennett, K.C.; Berla, L.A.; Nix, W.D.; Borja, R.I. Instrumented nanoindentation and 3D mechanistic modeling of a shale at multiple scales. *Acta Geotech.* **2015**, *10*, 1–14. [CrossRef]
81. Yang, T. Research on micromechanical properties of breccia based on atomic force microscope. *Fly Ash Compr. Util.* **2022**, *36*, 29–35. [CrossRef]
82. Zhang, M.; Zhang, G.; Du, X. Characterization of Fracture Process in Shale: Insights From Micro-Scale DIC. In Proceedings of the 55th U.S. Rock Mechanics/Geomechanics Symposium, Virtual, 20–23 June 2021; p. ARMA–2021-1747.
83. Nath, F.; Aguirre, G.; Aguirre, E. Characterizing Complex Deformation, Damage, and Fracture in Heterogeneous Shale Using 3D-DIC. *Energies* **2023**, *16*, 2776. [CrossRef]
84. Githens, A.; Ganesan, S.; Chen, Z.; Allison, J.; Sundararaghavan, V.; Daly, S. Characterizing microscale deformation mechanisms and macroscopic tensile properties of a high strength magnesium rare-earth alloy: A combined experimental and crystal plasticity approach. *Acta Mater.* **2020**, *186*, 77–94. [CrossRef]
85. Zhang, S.; Godfrey, A.; Zhang, C.; Liu, W.; Juul Jensen, D. Surface patterning for combined digital image correlation and electron backscatter diffraction in-situ deformation experiments. *Mater. Charact.* **2020**, *164*, 110332. [CrossRef]
86. Caduff, D.; Van Mier, J.G.M. Analysis of compressive fracture of three different concretes by means of 3D-digital image correlation and vacuum impregnation. *Cem. Concr. Compos.* **2010**, *32*, 281–290. [CrossRef]
87. Gao, G.; Yao, W.; Xia, K.; Li, Z. Investigation of the rate dependence of fracture propagation in rocks using digital image correlation (DIC) method. *Eng. Fract. Mech.* **2015**, *138*, 146–155. [CrossRef]
88. Roux, S.; Hild, F. Stress intensity factor measurements from digital image correlation: Post-processing and integrated approaches. *Int. J. Fract.* **2006**, *140*, 141–157. [CrossRef]
89. Zhao, Y.; Ma, S. Deformation Field around the Stress Induced Crack Area in Sandstone by the Digital Speckle Correlation Method. *Acta Geol. Sin.* **2009**, *83*, 661–672. [CrossRef]
90. Dautriat, J.; Bornert, M.; Gland, N.; Dimanov, A.; Raphanel, J. In-situ analysis of strain localization related to structural heterogeneities of carbonate rocks. *EPJ Web Conf.* **2010**, *6*, 1–23. [CrossRef]
91. Dautriat, J.; Bornert, M.; Gland, N.; Dimanov, A.; Raphanel, J. Localized deformation induced by heterogeneities in porous carbonate analysed by multi-scale digital image correlation. *Tectonophysics* **2011**, *503*, 100–116. [CrossRef]
92. Renard, F.; McBeck, J.; Kandula, N.; Cordonnier, B.; Meakin, P.; Ben-Zion, Y. Volumetric and shear processes in crystalline rock approaching faulting. *Proc. Natl. Acad. Sci. USA* **2019**, *116*, 16234–16239. [CrossRef]
93. Wenk, H.R.; Houtte, P.V. Texture and anisotropy. *Rep. Prog. Phys.* **2004**, *67*, 1367. [CrossRef]
94. Stipp, M.; Stünitz, H.; Heilbronner, R.; Schmid, S.M. The eastern Tonale fault zone: A 'natural laboratory' for crystal plastic deformation of quartz over a temperature range from 250 to 700 °C. *J. Struct. Geol.* **2002**, *24*, 1861–1884. [CrossRef]
95. Mansouri, H.; Prior, D.J.; Ajalloeian, R.; Elyaszadeh, R. Deformation and recrystallization mechanisms inferred from microstructures of naturally deformed rock salt from the diapiric stem and surface glaciers of a salt diapir in Southern Iran. *J. Struct. Geol.* **2019**, *121*, 10–24. [CrossRef]
96. Belytschko, T.; Black, T. Elastic crack growth in finite elements with minimal remeshing. *Int. J. Numer. Methods Eng.* **2015**, *45*, 601–620. [CrossRef]
97. He, J.; Zhang, Z.; Li, X. Numerical Analysis on the Formation of Fracture Network during the Hydraulic Fracturing of Shale with Pre-Existing Fractures. *Energies* **2017**, *10*, 763. [CrossRef]
98. Nagel, N.; Sanchez-Nagel, M.; Zhang, F.; Garcia, X.; Lee, B. Coupled Numerical Evaluations of the Geomechanical Interactions Between a Hydraulic Fracture Stimulation and a Natural Fracture System in Shale Formations. *Rock Mech. Rock Eng.* **2013**, *46*, 581–609. [CrossRef]
99. Shi, G. Discontinuous Deformation Analysis: A New Numerical Model for the Statics and Dynamics of Deformable Block Structures. *Eng. Comput.* **1992**, *9*, 157–168. [CrossRef]
100. Stolarska, M.; Chopp, D.L.; MoS, N.; Belytschko, T. Modelling crack growth by level sets in the extended finite element method. *Int. J. Numer. Methods Eng.* **2001**, *51*, 943–960. [CrossRef]
101. Zhou, L. A new numerical 3D-model for simulation of hydraulic fracturing in consideration of hydro-mechanical coupling effects. *Int. J. Rock Mech. Min. Sci.* **2013**, *60*, 370–380. [CrossRef]
102. Gao, F.; Stead, D. The application of a modified Voronoi logic to brittle fracture modelling at the laboratory and field scale. *Int. J. Rock Mech. Min. Sci.* **2014**, *68*, 1–14. [CrossRef]
103. Kazerani, T.; Zhao, J. Micromechanical parameters in bonded particle method for modelling of brittle material failure. *Int. J. Numer. Anal. Methods Geomech.* **2010**, *34*, 1877–1895. [CrossRef]
104. Ghazvinian, E.; Diederichs, M.S.; Quey, R. 3D random Voronoi grain-based models for simulation of brittle rock damage and fabric-guided micro-fracturing. *J. Rock Mech. Geotech. Eng.* **2014**, *6*, 506–521. [CrossRef]
105. Wang, X.; Cai, M. Modeling of brittle rock failure considering inter- and intra-grain contact failures. *Comput. Geotech.* **2018**, *101*, 224–244. [CrossRef]
106. Li, X.; Li, H.; Zhao, J. 3D polycrystalline discrete element method (3PDEM) for simulation of crack initiation and propagation in granular rock. *Comput. Geotech.* **2017**, *90*, 96–112. [CrossRef]
107. Bewick, R.; Kaiser, P.; Bawden, W. DEM Simulation of Direct Shear: 2. Grain Boundary and Mineral Grain Strength Component Influence on Shear Rupture. *Rock Mech. Rock Eng.* **2014**, *47*, 1673–1692. [CrossRef]

108. Bewick, R.; Kaiser, P.; Bawden, W.; Bahrani, N. DEM Simulation of Direct Shear: 1. Rupture Under Constant Normal Stress Boundary Conditions. *Rock Mech. Rock Eng.* **2013**, *47*, 1647–1671. [CrossRef]
109. Potyondy, D. A grain-based model for rock: Approaching the true microstructure. *Itasca* **2010**, *1*, 1–9.
110. Abdelaziz, A.; Zhao, Q.; Grasselli, G. Grain based modelling of rocks using the combined finite-discrete element method. *Comput. Geotech.* **2018**, *103*, 73–81. [CrossRef]
111. Ji, L.; Lin, M.; Cao, G.; Jiang, W. A core-scale reconstructing method for shale. *Sci. Rep.* **2019**, *9*, 4364. [CrossRef]
112. Li, X.; Li, H.; Zhao, J. The role of transgranular capability in grain-based modelling of crystalline rocks. *Comput. Geotech.* **2019**, *110*, 161–183. [CrossRef]
113. Maerten, L. Variation in slip on intersecting normal faults: Implications for paleostress inversion. *J. Geophys. Res.* **2000**, *105*, 25553–25565. [CrossRef]
114. Maerten, L.; Maerten, F. Chronologic modeling of faulted and fractured reservoirs using geomechanically based restoration: Technique and industry applications. *AAPG Bull.* **2006**, *90*, 1201–1226. [CrossRef]
115. Maerten, L.; Maerten, F.; Lejri, M.; Gillespie, P. Geomechanical paleostress inversion using fracture data. *J. Struct. Geol.* **2016**, *89*, 197–213. [CrossRef]
116. Zhang, W.; Chen, Y.-Y.; Guo, J.-P.; Wu, S.-S.; Yan, C.-Y. Investigation into Macro- and Microcrack Propagation Mechanism of Red Sandstone under Different Confining Pressures Using 3D Numerical Simulation and CT Verification. *Geofluids* **2021**, *2021*, 2871687. [CrossRef]
117. Mehdikhani, M.; Aravand, M.; Sabuncuoglu, B.; Callens, M.G.; Lomov, S.V.; Gorbatikh, L. Full-field strain measurements at the micro-scale in fiber-reinforced composites using digital image correlation. *Compos. Struct.* **2016**, *140*, 192–201. [CrossRef]